Mid-infrared spectroscopy of starbursts : from Spitzer-IRS to JWST-MIRI

Martínez-Galarza, J.F.

CHAPTER 1

Introduction

The Spectral Energy Distributions (SEDs) of star-forming regions and starburst galaxies are unique tracers of the star formation processes in these environments, since they contain information on the escaping and processed photons emitted by newly formed massive stars. Understanding these internal processes is crucial in our physical interpretation of observations of unresolved star formation in the Universe. In the first part of this thesis, we study the physical conditions in resolved starburst regions using Bayesian fitting of their spatially integrated infrared SEDs, including both the thermal continuum and the atomic emission lines. We then apply the method to unresolved starburst to learn about their star formation physics. Our approach leads to robust constraints on physical parameters such as age, compactness, and amount of currently ongoing star formation in starburst, which are otherwise biased by model degeneracies, and allows us to link the resolved properties of giant H $\scriptstyle\rm II$ regions to the star formation process at larger scales. In the second part of this thesis, we discuss the wavelength calibration of the next instrument to study the mid-infrared spectral properties of starbursts, with improved resolution and sensitivity: the mid-infrared instrument (MIRI), which will fly onboard the *James Webb Space Telescope* in 2018.

1.1 Massive star formation and the history of the Universe

The process through which large amounts of gas and dust in Giant Molecular Clouds (GMCs) are turned into crowded populations of stars with total masses of between $10^4 M_\odot$ and $10^6 M_\odot$ is a crucial problem in astrophysics. It is related to the structure of the Universe as we see it today, with all the complexity and beauty revealed by optical and infrared telescopes at scales ranging from the size of individual stars to the majestic structures of entire spiral galaxies. The most massive OB stars formed within these clusters affect the structure of galaxies through their radiative and mechanical input and through the chemical processing of the interstellar medium (ISM), thus influencing the evolution of the galaxy as a whole. The incidence of star formation in the evolution of galaxies was even more important at earlier times, when young gas-rich galaxies were in the process of assembling (Caputi et al. 2007). In fact, deep near-infrared surveys indicate that about 85% of all the baryonic mass that exists today in galaxies was formed in the last 9 billion years in massive star forming regions heavily embedded in thick layers of dust (Marchesini et al. 2009).

These facts highlight the importance of understanding the formation of massive star clusters both in the local and distant Universe, and their evolution during the first ~ 10Myr of their existence, when the bulk of ultraviolet (UV) radiation from OB stars is emitted. Dedicated theoretical and observational efforts have been made to characterize the initial physical conditions for the formation of large stellar clusters in GMCs (see the review by Zinnecker & Yorke 2007, and references therein), and also the early stages of embedded clusters within these clouds (see for example Lada & Lada 2003, for a comprehensive review on embedded clusters in GMCs). As summarized in these reviews, most observational efforts have concentrated on tracing emission from: *(a):* the molecular gas that constitutes the fuel for the formation of massive stars, using submillimeter and radio observations of tracers of dense cores, such as HCO^+; and HCN and *(b):* thermal emission from dust particles heated by the intense radiation fields of young stars, using infrared imaging and spectroscopy.

In recent years, the study of the interaction between the radiation field of young OB stars formed within the cluster and the surrounding ISM, has benefited from new observations at mid-infrared and far-infrared observations, that complement previous optical and sub-millimeter surveys. It is now possible to sample the pan-chromatic spectral energy distributions (SEDs) of star-forming regions, from the UV to the far-infrared (FIR). These SEDs are dominated by the radiation field of OB stars that either escapes the birth cloud or is absorbed and processed by the gas and dust in the surrounding ISM. Because OB stars are short-lived, the SEDs provide information on the recent (< 10 Myr) star formation activity in these regions. In fact, for spatially unresolved objects, integrated SEDs are often the only diagnostic available to study their properties. The main goal of this thesis is the design of a robust method to derive physical information from the integrated SEDs of star-forming regions. Although we apply the method to regions with high specific star formation rates, the algorithms developed here should be suitable for any region whose

luminosity is dominated by star formation.

1.2   Starbursts systems

Star formation does not occur at the same rate everywhere in the local Universe. While most present day galaxies, including our Milky Way, have star formation rates (SFRs) of $\sim$ 1 $M_\odot$ yr^{-1} (Robitaille & Whitney 2010), a minority of local galaxies with similar stellar masses are undergoing bursts of star formation, and have SFRs of hundreds or even thousands of solar masses per year. While it is not entirely clear yet what triggers these *starbursts*, galaxy mergers have been proposed as a possible (but not unique) cause for the enhanced star formation (Sanders & Mirabel 1996). This is supported by the fact that the total contribution from luminous infrared galaxies to the cosmic SFR density is larger at higher redshifts, where collisions between galaxies were more common (Lagache et al. 2005). Fig. 1.1 shows the SEDs of different types of galaxies and provides evidence for the pronounced infrared emission from star-forming galaxies with respect to normal disk galaxies.
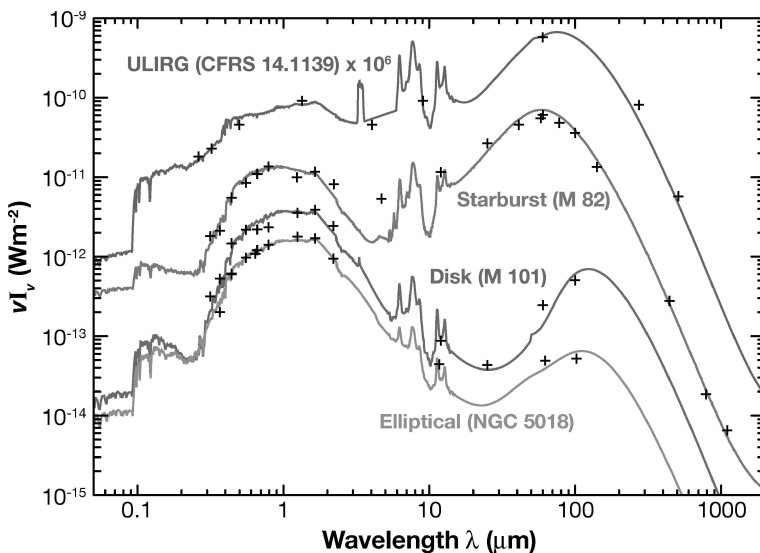
Figure 1.1 The UV to FIR SEDs of different galaxy types, from elliptical dust-poor galaxies to Ultra Luminous Infrared Galaxies (ULIRGs). The crosses indicate photometry data, while the solid lines are SED models. Figure taken from Galliano (2004).

1.2.1   Definition of a starburst

The term *starburst* has been used by astronomers for about 40 years. The first reference in the scientific literature to *bursts* of star formation in galaxies comes from the seminal paper by Searle et al. (1973). In that paper, the authors claim that transient periods of enhanced star formation could be one possible explanation for the colors of certain galaxies, which were observed to be bluer than expected, indicating a young population of massive stars. Almost a decade later, (Weedman et al. 1981) used the term *starburst* for the first time, referring to the intense nuclear star formation activity in NGC 7714, as estimated using X-ray, optical and radio data. However, due to the broad interval of wavelengths at which massive star formation is detected, and to the equally spread range of bolometric luminosities of objects classified as starbursts (10^8 L$_\odot$ − 10^{12} L$_\odot$), no formal definition of a starburst has been adopted, leading to confusion in the understanding of their nature.

Nevertheless, it is generally agreed that if such definition is to be adopted, it should be related to the following three factors: *(i):* The SFR of the galaxy or region, *(ii):* The amount of available gas to form stars, and *(iii):* The timescale of star formation as compared to the dynamical timescales of the system (e.g., galactic rotation period). A possible definition that includes these concepts was introduced by Heckman (2005). According to this definition, a starburst is a system in which the timescale t_{gas} for gas depletion is much shorter than the Hubble time. This can be written in an equation as

$$t_{\mathrm{gas}} = M_{\mathrm{gas}}/\mathrm{SFR} << 1/\mathrm{H}_0 \qquad (1.1)$$

where M_{gas} is the mass of molecular gas in the system, measured for example using radio observations of molecular tracers such as CO, SFR is the star formation rate as estimated from optical or infrared diagnostics, and H_0 is the Hubble constant.

We can classify systems with different star formation intensities using this definition. For the Milky Way, $t_{\mathrm{gas}} \sim 3$ Gyr, while for two well known local galactic mergers, M82 and Arp 220 (see Fig. 1.2), we have respectively $t_{\mathrm{gas}}^{\mathrm{M82}} \sim 20$ Myr and $t_{\mathrm{gas}}^{\mathrm{Arp220}} \sim 30$ Myr, as estimated from literature values for their masses and SFRs. This indicates that the latter two can be included in the category of starbursts. The definition is not exclusive of galaxies. A gas depletion timescale can also be used to classify star forming regions within galaxies, such as the 30 Doradus region in the Large Magellanic Cloud, for which $t_{\mathrm{gas}}^{\mathrm{30Dor}} \sim 10$ Myr.

A different approach considers the starburst bolometric luminosity, L_{SB}, as compared to the luminosity of the galactic host, L_{G} (Terlevich 1997). Bolometric luminosities are usually measured adopting template SEDs that are scaled according to available measurements, and then integrated within a certain wavelength range. According to this alternative definition, a galactic system is a starburst galaxy if $L_{\mathrm{SB}} >> L_{\mathrm{G}}$. This approach avoids ambiguities arising from uncertainties in the total gas mas, but excludes in the definition star forming regions such as 30 Doradus.

Figure 1.2 The starburst galaxy Arp 220 as seen by the *Hubble Space Telescope*. The bright blue spots are young clusters whose formation was triggered by the galactic collision. The light of many more clusters is obscured by large amounts of dust in the foreground. Image from Wilson et al. (2006).

1.2.2 Giant H II regions as the building blocks of starbursts

Behind the thick layers of gas and dust in starburst systems, stars form inside individual clouds with a distribution of masses set by the physical conditions of the molecular cloud before its collapse (see, for example Motte et al. 1998). The most massive (OB) stars in the resulting clusters are hot and luminous enough to ionize the surrounding gas, creating extensive H II regions (see, for example Shields 1990,for a review on H II regions). The ionized gas then tends to expand, dispersing the parental molecular cloud and creating a shock front into the surrounding neutral molecular gas. These so-called Giant H II Regions (GH IIRs) are thus the building blocks of starburst systems, not only because they represent the self-contained systems of star formation of which the starburst is made, but also because through their mechanical and radiative feedback, they alter the evolution of the starburst, setting a limit to the efficiency at which the molecular gas can be converted into stars (Krumholz et al. 2006). In Fig. 1.3 we show an simple schematic 2D view of an H II region.

Infrared bright clumps are usually observed in the vicinity of H II regions, and this has been generally associated with star formation triggered by the compressed gas as the expansion of the ionized region progresses (see Elmegreen 2011, and references therein).
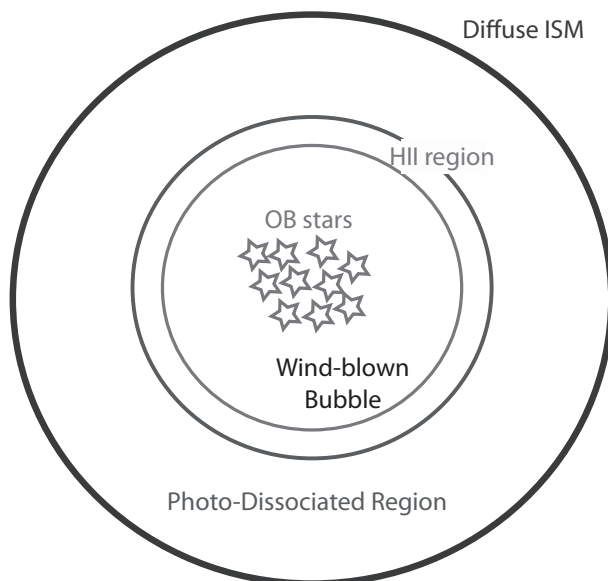
Figure 1.3 An schematic view of a symmetric H II region. The hot central stars expand, creating a cavity of shocked gas surrounded by a thing layer of ionized gas. Photons with energies below the ionization potential of the hydrogen atom process the surrounding molecular material, creating a photon-dominated region (PDR), that diffuses into the ISM. Figure by Brent Groves.

Possible evidence has been found of triggered intermediate-mass star formation in galactic regions of massive star formation, such as the RCW 34 region in the Vela Molecular Ridge (Bik et al. 2010). Nonetheless, not enough observational evidence for triggering of new massive stars has been collected, mainly due to weak indicators of ongoing massive star formation in galactic systems. It is in general difficult to judge whether very recent star formation events have taken place before or after the disturbance in pressure created by an expanding H II region. Triggering can be responsible for a significant contribution to the starburst activity, and hence quantifying it in the interior of star-forming regions is crucial in our understanding of these systems. In this thesis, we will quantify recent massive star formation in the vicinity of GH II Rs by fitting their integrated SEDs with a novel statistical method.

Infrared Observations of GH II Rs

Because massive star formation occurs in regions heavily enshrouded by dust, a significant fraction of their bolometric luminosity is emitted at infrared wavelengths, after UV photons from massive stars have been absorbed by dust particles and re-emitted as ther-

mal radiation (see Fig. 1.1). In fact, the total IR luminosity of a galaxy can be used as a tracer of its recent star formation history (Kennicutt 1998, Calzetti et al. 2010). Apart from the thermal continuum, several relevant features are observed at the wavelengths covered by recent infrared observatories including the *Spitzer Space Telescope* and the *Herschel Space Observatory*.

At mid-infrared (MIR) wavelengths (5 μm-28 μm), the SEDs of starbursts are dominated by pronounced and broad emission features arising from bending and stretching mode transitions in Polycyclic Aromatic Hydrocarbons (PAHs) (Tielens 2008). These are molecules with carbon atoms arranged in a honeycomb structure of fused six-membered, aromatic rings with peripheral hydrogen atoms. These PAHs are present in the molecular photon-dominated regions (PDRs) that surround H II Regions. Atomic fine-structure emission lines from several highly ionized species including [Ar III], [S IV] and [Ne III] are also detected in the MIR and are important tracers of gas density, temperature and strength of the radiation field (Dopita et al. 2006c). Additionally, the prominent [Si II] line detected in the MIR spectrum of many galaxies traces either gas shocked by supernova explosions, or regions dominated by the X-rays in the stellar winds of massive stars. None of these species are present in low-mass star-forming regions, where the radiation fields are not as intense.

Fig. 1.4 illustrates the complexity of starbursts as revealed by their MIR spectra. Shown are the spectra of a sample of starburst galaxies taken with the Infrared Spectrograph (IRS) onboard *Spitzer*, which display a wide range in the strength of MIR features and continuum slopes (Brandl et al. 2006). Understanding how the underlying physics of star-forming regions relate to the observed spectral features is one of the goals of the present work.

Observations at even longer wavelengths allow a first order approach to the measurement of the average dust temperature and total amount of dust contained in starbursts (and hence of their evolutionary stage), by characterizing the peak and broadness of the thermal radiation bump observed at far-infrared (FIR) wavelengths. Although such physical quantities are biased by uncertainties in the SED models (dependence of dust emissivity on the composition, degeneracy between the spectral index β and the dust temperature), some general relations can be established between starburst activity and the overall shape of the SED.

In a recent comprehensive paper on star-forming galaxies using *Herschel* data, Elbaz et al. (2011) characterized the SEDs of a sample containing $\sim$ 1800 galaxies, and concluded that they can be separated in two classes, according to their SED shapes. A majority of "main sequence" star-forming galaxies, with SFRs compared to that of the Milky Way and infrared bumps peaking $\sim$ 100 μm, and a minority of outliers whose SEDs peak at $\sim$ 70 μm that the authors associate with objects undergoing compact starburst-like star formation. Relating their overall SEDs to the internal conditions of their individual GH IIRs is an important step in the understanding of the physical processes that lead to the formation of a starburst. In the chapters of this thesis we will show that it is possible to constrain the average physical parameters of H II regions by fitting the integrated SED of the starburst galaxy that hosts them.

The majority of starburst galaxies are distant and spatially unresolved by our current
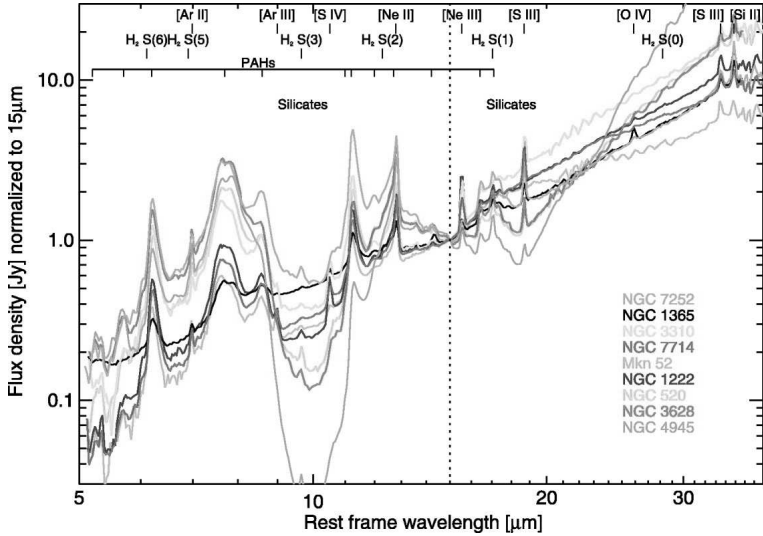
Figure 1.4 The MIR spectra of a sample of starburst galaxies, displaying a broad range of variation in the PAH strength, silicate absorption, slope continuum and atomic line emission. Some relevant MIR emission lines are indicated. Figure taken from Brandl et al. (2006).

instruments. Hence, in order to understand their internal properties, we rely almost exclusively on their integrated SEDs. Fig. 1.5 illustrates the situation, by showing the typical size of the galaxies whose SEDs are shown in Fig. 1.4 as compared to the size of the *Spitzer*-IRS slit. It is evident from the figure that most of the infrared emission from these objects is spatially unresolved. In the near future, the MIRI instrument for the *James Webb Space Telescope* (JWST) will move one step forward in resolution and sensitivity of mid-infrared observations (see in Chapters 5 and 6). However, even when MIRI comes online towards the end of the decade, resolved observations of individual GH ɪɪRs at mid-infrared wavelengths will not be possible at distances larger than about 30 Mpc. In terms of the science presented in this thesis, this implies that the method developed here will remain a powerful and unique tool to study unresolved starburst beyond the Local Universe, long after the JWST mission has been completed.

Modelling of H ɪɪRs and starbursts

From UV to submillimeter wavelengths, the emission properties of starbursts are dominated by the energetic photons emitted by massive stars younger than 10 Myr formed in OB associations and clusters (Kennicutt 1998). These photons are either directly observed as UV light or re-processed by gas and dust and re-emitted as atomic recombination lines or infrared thermal continuum. From the modelling point of view, this implies that the
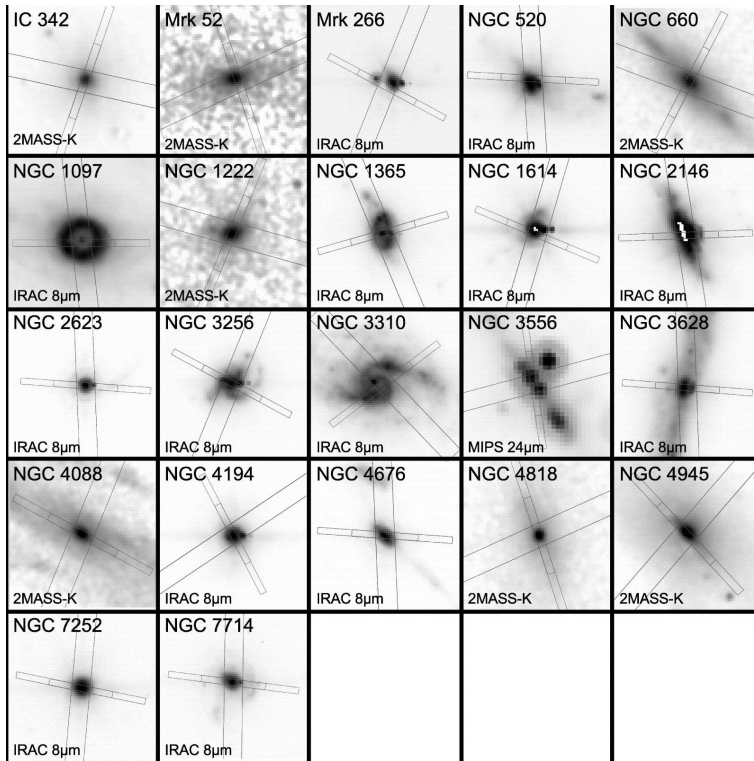
Figure 1.5 Positions of the *Spitzer*-IRS SL and LL slits overplotted on IRAC 8 μm, MIPS 24 μm, or 2MASS K-band images for a sample of starburst galaxies. Figure taken from Brandl et al. (2006).

SED of a starburst is constructed from the linear combination of the SEDs of the individual GH ɪɪRs created by those clusters, and their surrounding molecular envelopes. To first approximation, the physical modelling of such regions needs to account for at least three main components:

1. The time-dependent radiation field emitted by the photospheres of a given population of stars, which provides the energetic input for the system. This is the stellar population synthesis.

2. The physics of the interaction between the stellar radiation and the surrounding ISM. This is the ionization, excitation and radiative transfer part of the analysis.

3. The dynamical evolution of the H ɪɪ regions, which is driven by the competition between the radiation pressure that expands the H ɪɪ region and the external ISM pressure that confines it.

1 Introduction

To first approximation, a galaxy is a collection of stars that ranges from low-mass stellar objects to the massive and luminous OB stars, with a given distribution of ages and metallicities. The so-called Initial Mass Function (IMF), describes the distribution of masses with which a stellar cluster is born, and sets many aspects of its subsequent evolution. Population synthesis is the art of creating a galactic SED as the sum of the spectra of these individual stars, by parametrizing the evolution of the system either as a function of age (Charlot & Bruzual 1991) or as a function of available thermonuclear fuel (Maraston 2005). Stellar synthesis models simplify the physical situation by assuming ensembles of single-age and single-metallicity stellar populations with a time-dependant mass distribution. The output of the stellar population synthesis is the radiation field that is later used as an input for the radiative transfer analysis.

In order to account for the entire UV to sub-millimeter spectral energy distribution of galaxies, the stellar spectra are only the first step. It is necessary to account for the absorption of stellar light by gas and dust particles present in the ISM, and for the cooling radiation of the gas, heated by the absorption of stellar photons and/or by the photoelectric heating and collisions with the dust. Although dust and gas are mixed within the ISM, the radiative transfer is usually done separately for each of these components, since they have different absorption and emission properties. While for most star-forming regions the gas is assumed to be atomic, in very dense regions such as AGN-dominated galaxies and very luminous starbursts, molecular gas can be responsible for significant absorption of stellar light. Full radiative transfer codes accounting for ionization and excitation such as *CLOUDY* (Ferland et al. 1998) and *Mappings* III (Groves et al. 2008) compute the absorption of EUV photons with energies $hv > 13.6$ eV, and their re-emission as hydrogen recombination lines or collisionally excited forbidden lines of other atomic species. Additionally, these codes compute the absorption and emission of dust particles, which are considered to be made of three different components: amorphous graphite grains, amorphous silicate grains and PAHs (Mathis et al. 1977, Draine 2011).

As the stellar populations ages, the ionized H II region expands driven by the mechanical input of stellar winds and supernovae in the clusters. A one-dimensional approach to compute the dynamical evolution of this expansion was proposed by Castor et al. (1975), and refined by Oey & Clarke (1997) to account for superbubbles created by clusters of OB stars rather than individual stars. Using their approach, it is possible to derive the evolution of the H II region radius as a function of only two parameters: the mechanical energy from stellar winds and supernovae as a function of time, which comes from the stellar synthesis analysis, and the density of the surrounding ISM, which provides the confining pressure against which the bubble expands. While this one-dimensional approach is a simplification of the more complex geometry of these systems, it provides values that can be directly compared with observations of expanding bubbles in the galaxy, such as the observed radii of such bubbles.

1.3 SED fitting of starbursts

One of the most common and wide-spread methods used in the last decade to determine the physical conditions of unresolved starbursts and of star-forming regions in general, is the fitting of observed SEDs using pre-calculated models like those described in the last section. This has been possible given major improvements in both physical models and the fitting procedures in recent years, as described in a comprehensive review by Walcher et al. (2011). By comparing the observed spectrum to predicted SEDs from models in which the physical conditions have been parametrized, one should be able to find a set of model parameters that better reproduce the data, given certain observational uncertainties, and hence derive probability distributions for the model parameters. Some of the important parameters to be constrained are the SFRs, age, compactness of the regions, mass contribution from young embedded objects, and PDR content.

1.3.1 χ^2 minimization

Most of the fitting techniques used today are based on χ^2 minimization routines that measure the difference between observed and predicted spectra in a bin-by-bin basis (along the frequency axis) and compare this difference to the observational error for each corresponding wavelength bin. It is then possible to obtain a distribution of χ^2 values for the model parameters by calculating this quantity across the full parameters space. It is assumed that the set of parameter values that minimize the χ^2 distribution is a good representation of the actual values of the physical quantities.

These minimization methods assume that the model parameters are fixed but unknown, and that the uncertainties in their determination are given by the *likelihood* of measuring certain values for the parameters assuming that the adopted models are a fair representation of reality. If the observational errors are distributed according to a Gaussian, this likelihood probability can be calculated as the exponential of the χ^2 distribution arising from the comparison between the possible outcomes of the models and the observed data, the *evidence*. In this respect, χ^2 minimization methods are *frequentist* in that they assume that the probability of a given model parameter having a certain value is determined by the spread in the results of applying a test (the SED fitting) to the measurement of a fixed parameter.

An important aspect of χ^2 minimization is that in order to provide reliable results, it requires a thorough mapping of the parameter space in order to avoid local shallow minima that can be misleading.

1.3.2 Bayesian approach

A more sophisticated, and philosophically different approach assumes that the model parameters are not fixed quantities, but random variables whose probability distribution functions (PDFs) are set, before any attempt of measurement has been made, by the belief of the scientist that the model parameters have certain values. These beliefs should

be based on independent knowledge of the parameters, either from observations or theory, and constitute probability *priors* for the model parameters. In Bayesian inference, we measure the *posterior* probability distribution of a given parameter by updating its assumed prior probability in the light of new evidence. This evidence comes from new observations (the measured spectrum of a star-forming region, for example) and enters the calculation as the likelihood derived from the χ^2 minimization. The Bayes' theorem relates the posterior PDF to the likelihood and prior probabilities according to:

$$\text{posterior} = \text{likelihood} \times \text{prior} \times \frac{1}{N} \tag{1.2}$$

where N is a normalization factor that ensures that the posterior adds up to unity.

An advantage of Bayesian inference over frequentist methods is that it allows to update our previous knowledge on a particular model parameter using any new evidence on that particular parameter. Moreover, via the normalization constant, it accounts for the fact that SED fitting is nothing but a test, and as such it might detect things that do not exist (*false positives*) or fail to detect things that do exist (*false negatives*). Bayesian inference is, from the point of view of the author of this thesis, the right method to use when one is trying to calculate the probabilities of model parameters about which enough evidence has been collected prior to the measurements.

1.4 Future observations with the James Webb Space Telescope

The level of detail with which we can study the MIR SEDs of star-forming galaxies is limited by the sensitivity, angular resolution and spectral resolving power of our current spectroscopic observations. In particular, at wavelengths longer than 5 μm, the spectra of star-forming galaxies located at distances larger than a few tens of Mpc are either dimmer than the current detection limits ($\sim$ 1 mJy with *Spitzer*-IRS) or spatially unresolved by the beam size of the available imaging devices ($\sim$ 1''.7 for *Spitzer*-IRAC at 8 μm), with the exception of very bright objects. Moreover, the current spectral resolutions achieved at MIR wavelengths do not exceed values of $\lambda/\Delta\lambda \sim$ 600. The sensitivity and angular resolution limitations can be overcome with a larger aperture telescope optimized for MIR wavelengths, which combined with state-of-the-art spectroscopic techniques, can also provide better spectral resolution.

1.4.1 JWST

Towards the end of the decade, a 6.5 m infrared-optimized telescope will be launched to the so-called Lagrange point No. 2, located at a distance of 150 million kilometers from the Earth, that offers a privileged observing location far from the thermal radiation of the Earth-Moon system. The *James Webb Space Telescope* (JWST) is a joint effort of three space agencies, namely NASA, ESA, and the Canadian Space agency and will constitute

the next milestone in space-based infrared astronomy. With an effective collecting area 40 times as big as that of the *Spitzer* main mirror, it will reach unprecedented sensitivity at wavelengths ranging from 0.6 μm to 29 μm using four observing instruments: a 2.2′×4.4′ field near-infrared camera, a near-infrared multi-object dispersive spectrograph with a field of view of 3.4′×3.4′, a 2.2′×2.2′ tunable filter imager and a mid-infrared instrument that will perform imaging, coronagraphy and integral field spectroscopy.

1.4.2   Sensitivity

The unprecedented dimensions of JWST imply that it will be able to perform observations two orders of magnitude more sensitive at MIR wavelengths as compared to the *Spitzer* Space Telescope, limited only by the thermal background from the telescope itself, and by the IR background from galactic cirrus. In fact, the telescope is designed to observe the light from the first stars that formed in the history of the Universe, at redshifts larger than $z \sim 13$ (Stiavelli 2010). To detect these sources, JWST needs to be able to measure photometric flux densities as low as 10^{-8} Jy for a point source, at the 10-σ level in a 10^4 s exposure. This means that the telescope has to operate at extremely low temperatures, close to 40 K, and even lower ($\sim$ 7 K) for the mid-infrared instrument (MIRI), whose solid state detectors require such operating temperature. In Fig. 1.6 we show a comparison in the limiting flux densities for several observatories including JWST (6.5 m aperture), Spitzer (0.85 m), HST (2.4 m), the Gemini Telescopes (8.2 m) and the SOFIA observatory (2.5 m).

1.4.3   Spatial resolution

The diffraction-limited beam size of JWST varies with wavelength from 0.063″ at 2 μm to 0.635″ at 20 μm. The resolution elements are optimally sampled by at least 2 detector pixels. For comparison, the diffraction limit for the *Hubble* aperture is about 0.14″ at 2 μm and that of the *Spitzer* Space Telescope is 6.18″ at 24 μm. Observing in the MIR thermal continuum, JWST will be able to resolve the size of typical giant H II regions, such at 30 Doradus (200 pc), at the distance of the Virgo cluster of galaxies.

1.4.4   MIRI spectrometry

The JWST-MIRI instrument will have integral field spectroscopy capabilities with resolving powers ranging from $R \sim 1000$ to $R \sim 4000$ between 5 μm and 29 μm. Four spectrometer channels with nested fields of view (FOVs) will register the science target and the spectrometer optics will divide the FOVs into adjacent slices that will be aligned and then dispersed by a dedicated set of gratings. The maximum size of the FOV is 7.7″ × 7.9″. Both in terms of wavelength coverage and functionality, the MIRI spectrometer will be the natural successor to the *Spitzer*-IRS.
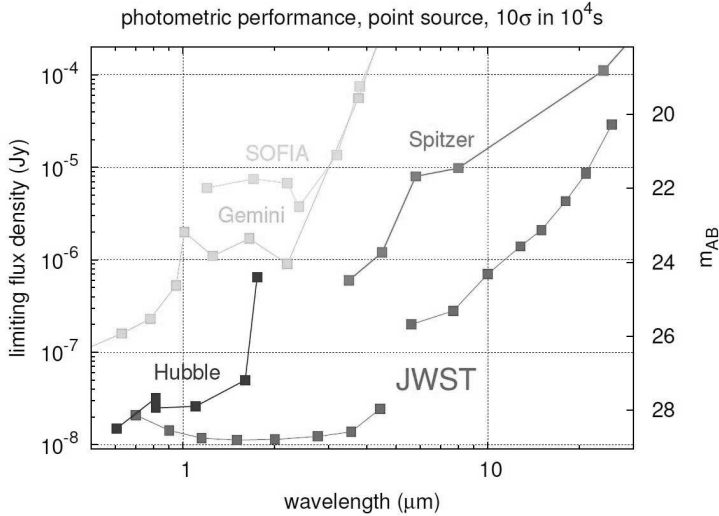
Figure 1.6 The faintest photometric flux of a point source that can be detected at 10σ in a 10^4 s integration, for different instruments observing at NIR and MIR wavelengths. JWST will be able to characterize the dimmest objects ever observed in the Universe. Credit: STScI.

1.4.5   Starbursts and MIRI

Several aspects of starbursts studies would greatly benefit from the large aperture of JWST, and from the imaging and spectroscopic capabilities of MIRI. In the Local Universe, at distances shorter than 30 Mpc, MIRI will be able to spatially resolve physical sizes of 45 pc (compared to about 300 pc resolved by previous infrared missions at the same distance), hence entering the domain of very compact nuclear starburst. We need MIRI to resolve this very inner regions of galactic nuclei, and to separated them from other galactic components or AGN. Additionally, MIRI will be able to penetrate through the dense layers of dust that obscures these nuclear starbursts. IFU spectroscopy of these regions will reveal with unprecedented spectral and spatial resolution several important features of the spectra that trace star formation, such as the PAH emission, and will allow detailed studies of the gas kinematics. Several MIR forbidden emission lines that are either dim or blended with other features will be readily detected. Some of those lines, such as the [O IV]25.89μm and the [Ne V]14.32μm can be used as discriminators between an active nucleus and a starburst nucleus.

At redshifts $z \sim 1$, the rest-frame near-infrared bands shift into the MIR wavelength range. MIRI will allow the measurement of stellar masses in intermediate z objects, based on their near-IR emission. The Paα near-infrared line at 1.87 μm shifts into the MIRI range for $z > 1.7$, allowing detailed kinematic studies of the ionized gas at kpc scales.

All together, these facts imply that more sensitive observations, with better angular resolutions, are needed to advance in the understanding of starbursts. MIRI will be provide these observational capabilities.

1.5   This thesis

Unveiling the physical mechanisms that trigger and maintain events of enhanced star formation in galaxies along the history of the Universe is one of the most exciting challenges of modern astrophysics. In this thesis we will study the physical conditions in star-forming regions, such as age, total mass, star formation rates, PDR content, pressure, and amount of ongoing massive star formation, using their integrated spectral energy distributions as indicators. The goal is to understand how and to what extent specific physical conditions affect the infrared SEDs of these objects in order to develop a robust SED fitting method that can be easily applied to any unresolved starburst and, more importantly, obtain reliable results on their physical conditions and their relation to star formation. As we have seen above, even with the next generation infrared instruments, most distant starbursts will still be unresolved, and physical modelling thus remains a crucial tool for the near future. Hence, in **Part** I of this thesis we develop a Bayesian approach to fit the integrated SEDs of starbursts and their emission lines with physical models. We apply the resulting tool to the infrared spectra of well known calibrators, the giant star forming regions 30 Doradus and NGC 604, before we use it to interpret the spectra of more distant, unresolved starbursts.

There is a reason why this thesis has two parts. The next milestone in observational studies of starbursts will be the launch of JWST in 2018. We have discussed several aspects of how the improved sensitivity, angular and spectral resolution of JWST-MIRI are needed to advance in our knowledge of these objects, both in the local and high-z Universe. MIRI observations will be directly linked to the science and methods discussed in this work. Therefore, **Part** II of this thesis is dedicated to MIRI, its performance and ground calibration before integration with the other observatory instruments. We introduces the MIRI instrument, and describe the ground calibrations of its spectral properties. Based on test data obtained during the testing of the instrument in Europe, we derive its wavelength calibration, and compare our results to the requirements set by the science goals of the mission.

In **Chapter 2** we present our novel Bayesian tool to fit the spectra of starbursts. The fitting tool is applied to the *Spitzer* spectrum of the giant H IIR 30 Doradus, a spatially resolved starburst. We find that our results are representative of this massive local starburst, and calibrate our tool using the wealth of literature information available for the region. Moreover, the model degeneracies are investigated. We discuss the importance of including the atomic nebular lines in the SED fitting in order to break these degeneracies. We show that emission from a significant amount of hot ($\sim 300\,\mathrm{K}$) dust is needed to reproduce the SED of 30 Doradus.

Using a combination of observational and analytical tools, including the brand-new Bayesian algorithm and multi-wavelength observations, **Chapter 3** presents a comprehen-

sive analysis of the physical conditions in the second most massive star-forming region in the Local Group after 30 Doradus, the NGC 604 region in the M 33 galaxy. Several massive (10^3 M$_\odot$ $-$ 10^4 M$_\odot$) embedded clusters with diameters of about 15 pc are identified within the region, most likely the early stages of very recent star formation. These clusters account for about 8% of the total stellar mass in the region. Our results indicate that, while NGC 604 is a more evolved H $\textsc{ii}$ region, as compared to its largest sibling 30 Doradus, star formation in NGC 604 is still ongoing, triggered by the earlier bursts.

We conclude the first part of the thesis in **Chapter 4**, an outlook chapter that presents a pilot study showing the power of our Bayesian tool to investigate the properties of spatially unresolved starbursts. We provide some encouraging clues about the conditions for the formation of massive star clusters in these nuclear starbursts. If confirmed, this clues may imply that the most massive clusters have formed in gas-depleted regions. Moreover, they may imply that the gas-poor systems where massive clusters form have large luminosity contributions from very recent massive star formation. This can be interpreted as evidence of positive feedback from the inferred massive clusters. We propose a systematic study of a large sample of starburst SEDs, using the present method, to corroborate our findings.

Part II of the thesis is dedicated to the Mid-Infrared Instrument for JWST. A method for the wavelength calibration of the instrument, based on the use of synthetic etalon lines, fringing pattern and optical modelling is presented in **Chapter 5** and applied to data collected during the testing of MIRI's verification model (VM). Once the method has been calibrated and verified during VM testing, in **Chapter 6** it is fully applied to the Flight Model (FM) data acquired during the FM test campaign in 2011. This constitutes the only spectral calibration measurements of the instrument before its launch on 2018. The measured resolving power of MIRI over the entire wavelength range confirms the requirements and agrees with the predicted values for the resolving power from the optical model. Our results imply an improvement of at least one order of magnitude with respect to the resolving power of the *Spitzer*-IRS spectrometer low resolution orders, and at least a factor of 3 with respect to the resolving power of the IRS high resolution orders.